Chapter 6

ApoE deficient inducible mast cell knockout mice: A new model to study the role of mast cells in atherosclerosis.

Manuscript in preparation

Daniël van der Velden[1,2]
H. Maxime Lagraauw[2]
Anouk Wezel[2]
René E.M. Toes[1]
Johan Kuiper[2]
Ilze Bot[2]

[1] Department of Rheumatology, Leiden University Medical Center, Leiden, The Netherlands.
[2] Division of Biopharmaceutics, Leiden Academic Centre for Drug Research, Leiden, The Netherlands.

Abstract

Objective

Atherosclerosis can be considered as a lipid-driven chronic inflammatory disease of the large- and medium sized arteries. Innate mast cells accumulate in the atherosclerotic lesion during its development and can take up to 6% of all nucleated cells in rupture prone lesions. In the past years, a number of experimental atherosclerosis studies have been performed in mice to unravel the contribution of mast cells and their mediators to atherogenesis. Frequently, mice have been used with alterations in the stem cell signaling pathway like the $Kit^{W\text{-}sh/W\text{-}sh}$ mice, which results in mast cell deficiency. However, it became evident that $Kit^{W\text{-}sh/W\text{-}sh}$ mice suffer from bystander defects such as neutrophilia. To study the development of atherosclerosis without these side effects, we used a mast cell inducible knockout mouse, the Red Mast cell Basophil (RMB) mouse, in which mast cell deficiency is independent of stem cell signaling.

Methods and Results

RMB mice were crossed with apoE deficient mice to obtain RMB-$apoE^{-/-}$ mice. In these mice, mast cells were depleted by intraperitoneal Diphtheria Toxin (DT) injection or PBS injection as a control. Directly after mast cell depletion, mice were placed on a western type diet to induce lesion development. Two weeks after the start of the diet, semi-constrictive collars were placed around the carotids followed by 4 additional weeks of WTD. At sacrifice, we did not detect any differences in body weight, total cholesterol levels or total leukocyte counts between mast cell depleted and competent groups. Histological analysis of the carotids showed a consistent depletion of mast cells after DT treatment, which coincided with a reduction in both lesion size and necrotic core area and an increased collagen content. Furthermore, we detected reduced levels of circulating IL-6 and TNFα in mast cell depleted mice.

Conclusions

In this current study we confirmed in a novel mouse model that mast cells contribute to the initiation phase of atherosclerotic lesion development.

Introduction

Mast cells are innate immune cells which are located throughout the body in peripheral tissues as skin, gut and within the vascular system [1]. Close to the external environment they are one of the first immune cells able to respond to invading pathogens. Mast cells are equipped with a variety of receptors that enables them to react within seconds to a number of stimuli. IgE-mediated activation is by far the most powerful activation pathway of mast cells, which results in the release of preformed mediators such as tryptase, chymase and histamine stored within the granules of the cell. The acute release of mediators is followed by the secretion of newly synthesized mediators including chemokines and cytokines [2]. The role of mast cells in allergy and hypersensitivity is well known, but more recent, also the contribution of mast cells to immune driven disorders such as rheumatoid arthritis and atherosclerosis has been identified [3–5].

Mast cells accumulate within atherosclerotic lesions at sites of plaque rupture, where they can be up to 6% of all nucleated cells [6]. The lesion contains a number of different stimuli such as endogenous toll like receptor (TLR) ligands and immune complexes that could potentially activate mast cells. For example, oxLDL-immune complexes are able to activate mast cells via FcγRs to release tumor necrosis factor (TNFα), interleukin 8 (IL-8) and monocyte chemotactic protein 1 (MCP-1), which may enhance the inflammatory response within the lesion [7]. Upon activation, mast cells can release proteases like chymase and tryptase that are able to degrade collagen as well as HDL and induce apoptosis of smooth muscle cells, which will induce and accelerate lesion destabilization [8–10]. Likewise, systemic mast cell activation leads to plaque growth and destabilization, which can be rescued by the administration of the mast cell stabilizer cromolyn [11]. Moreover, atherosclerosis-prone mice deficient for mast cells ($LDLr^{-/-}Kit^{W\text{-}sh/W\text{-}sh}$) develop smaller and more stable lesions compared to control $LDLr^{-/-}$ mice [12]. Although these studies demonstrate that mast cells contribute to atherosclerotic lesion development and destabilization, the use of $Kit^{W\text{-}sh/W\text{-}sh}$ mice is limited due to the fact that these mice with a defect in c-kit signaling suffer from several complications such as neutrophilia and expansion of splenic myeloid-derived suppressor cells [13–15]. To circumvent these undesired effects, mice have been developed in which mast cell deficiency is induced independently of SCF signaling, for example the carboxypeptidase A(Cpa3)-Cre; $Mcl\text{-}1^{fl/fl}$ mice, the mast cell protease 5 (Mcpt5)-$Cre^{+}iDTR^{+}$ mice and the Red-Mast cell-Basophil (RMB) mice [16–19]. Cpa3-Cre; $Mcl\text{-}1^{fl/fl}$ mice express Cre recombinase under control of Cpa3 promoter, which is combined with a floxed allele of the antiapoptotic factor. This combination results in deficiency in mast cells and a marked reduction in basophils. Recently, mice have been developed were mast cells can be depleted upon injection with diphtheria toxin (DT). Examples are the Mcpt5-$Cre^{+}iDTR^{+}$ mice and RMB mice that co-express the simian DT receptor together with proteins highly expressed by mast cells, which are for these two mouse models Mcpt5 and FcεRIβ, respectively. Administration of DT to these mice will causes apoptosis of all cells that express the DT receptor.

In the current study we used the RMB mouse model to study the role of mast cells in atherosclerosis. In this mouse model, the repopulation kinetics of basophils and mast cells after depletion with DT is shown to different. Basophils are depleted relatively shortly (<12 days), whereas systemic mast cell depletion is maintained for up to 2 months after the last DT injection [19]. We crossed these RMB mice with apoE$^{-/-}$ mice to create an inducible mast cell knockout on an atherosclerotic-prone background, creating the RMB-apoE$^{-/-}$. In this study we used this mouse model to characterize the contribution e of the mast cell to atherosclerotic lesion initiation.

Material & Methods

Mice

All animal work was performed conform the guidelines from the Directive 2010/63/EU of the European Parliament. Experiments were approved by the Leiden University Animal Welfare committee. The red mast cell and basophil mouse strain (RMB mice, official name: B6.Ms4a2tm1Mal) was provided by the laboratory of dr. P. Launay INSERM U1149, Paris, France [19]. These mice express the simian diphtheria toxin receptor under control of the promoter of the FcεRIβ gene. Injection of diphtheria toxin induces apoptosis of all FcεRIβ expressing cells, which are in mice only basophils and mast cells [20]. The RMB mice were crossed with apoE$^{-/-}$ mice to obtain atherosclerosis-prone RMB-apoE$^{-/-}$ mice.

To systemically deplete all FcεRIβ^{+} cells, RMB-apoE$^{-/-}$ mice were injected i.p. on day 1, 3 and 8 with 25 ng/g bodyweight DT (Diphtheria Toxin Unnicked, C. diphtheriae (Cat #322326, CalBiochem)). Two weeks before the start of the experiment, mice received either DT injections as described above to deplete FcεRIβ^{+} cells or PBS as a control. The efficiency of DT treatment to deplete mast cells was determined by both FACS analysis for circulating basophils (CD49b^{+}/FcεRI^{+}/IgE+) three days after last DT injection and by a mast cell staining in the carotids and hearts (CAE, Sigma) at end of the study.

At week 0 mice were fed a Western type diet (0.25% cholesterol and 15% cacao butter, SDS, Sussex, UK) for total 6 weeks. Two weeks after the start of Western type diet (WTD), perivascular collars were placed around both left and right carotid artery, which causes low shear stress and disturbed blood flow at the proximal side of the collar that results in endothelial activation, increased endothelial adhesion molecule expression and atherosclerotic lesion formation [21]. In short, mice were anaesthetized by subcutaneous injection of ketamine (60 mg/kg, Eurovet Animal Health, Bladel, The Netherlands), fentanyl citrate and fluanisone (1.26 mg/kg and 2 mg/kg respectively, Janssen Animal Health, Sauderton, UK) and a semi-constrictive collar was placed.

At sacrifice, mice were anaesthetized as described above and sacrificed via orbital exsanguination. Fixation through the left cardiac chamber was performed with phosphate-buffered saline (PBS). Subsequently, both common carotid arteries and the heart were excised and stored in 3.7% neutral-buffered formalin (Formal-fixx; Shandon Scientific Ltd, UK) for histological analysis. Serum was obtained for determination of cytokine and immunoglobulin levels. Splenocytes, blood and heart lymph nodes were isolated for FACS analysis of leukocytes.

Histology and morphometry

Carotid arteries and hearts were embedded in Tissue-Tek® O.C.T.™ compound (Sakura BV, The Netherlands) after which cryosections were prepared. Section of the carotid arteries were stained with hematoxylin-eosin (H&E) to

determine lesion size and necrotic core area (in μm^2) at the side of maximal stenosis. Lesions in the aortic root were quantified in Oil Red-O-stained sections. Mean lesion area (in μm^2) was calculated from 6 serial sections, starting at the appearance of the tricuspid valves.

Collagen content was determined by staining with picrosirius red and an enzymatic staining (CAE, Sigma-Aldrich, Germany) was used for the visualization of mast cells. Perivascular mast cells were counted manually by a blinded independent operator. The necrotic core size was defined as the a-cellular, debris-rich plaque area as percentage of the total plaque area. The atherosclerotic lesion areas and histological stainings of both carotids and aortic root were quantified using the Leica image analysis system, consisting of a Leica DMRE microscope coupled to a video camera and Leica Qwin Imaging analysis system (Leica Ltd, UK).

Flow cytometry

At sacrifice, blood was obtained in EDTA tubes and white blood cell (WBC), red blood cell (RBC) and platelets (PLT) were determined using an automated Sysmex XT-2000iV veterinary haematology analyzer (Sysmex orporation, Kobe, Japan). For flow cytometry analysis, erythrocytes were removed using a specific erythrocyte lysis buffer (0.15 M NH_4Cl, 10 mM $NaHCO_3$, 0.1 mM EDTA, pH 7.3).

Blood leukocytes were stained extracellular with four different stains to determine a) monocytes ($NK1.1^-$/$Ly6G^-$/$CD11b^{hi}$), inflammatory monocytes ($NK1.1^-$/$Ly6G^-$/$CD11b^{hi}$/$Ly6C^{hi}$/$CCR2^+$) and neutrophils ($NK1.1^-$/$Ly6G^{hi}$/$CD11b^{hi}$), b) basophils ($CD3^-$/$CD4^-$/$CD19^-$/$CD8^-$/$CD49b^+$/IgE^+/$CD117^-$), c) T cells ($CD3^+$/$CD4^+$), d) B-cells ($CD19^+$/$B220^+$). The different used antibodies are summarized in table 1. Antibodies were obtained from (eBiosciences, US). Flow cytometry analysis was performed on the FACSCantoII and obtained data was analyzed using FACSDiva software (BD Biosciences, US).

Table 1: Antibody panels used for flow cytometry analysis

Staining	FITC	PE	PerCP	APC	e-Fluor-450
A.	NK1.1 (Clone: PK136)	Ly6G (Clone: 1A8)	Ly6C (Clone: HK1.4)	CCR2 (Clone: 475301)	CD11b (Clone: M1/70)
B.	IgE (Clone: R35-72)	IgE (Clone: R35-72)	CD3/4/19/8 (dump channel)	CD49b (Clone: HMa2)	n/a
C.	CD44 (Clone: IM7)	CCR7 (Clone: 4B12)	CD8α (Clone: 53-6.7)	CD62L (Clone: MEL-14)	CD4 (Clone: GK1.5)
D.	IgM (Clone: II/41)	CD45RA (Clone: RA3-6B2)	CD19 (Clone: eBio1D3)	IgD (Clone: 11-26c)	CD5 (Clone: 53-7.3)

Serum analysis

Serum cytokine and immunoglobulin levels were determined using a commercially available ELISA kit (BD, US, Bethyl laboratories, US). All procedures were according to manufacturer's protocol.

Serum concentrations of total cholesterol was determined by enzymatic colorimetric assay according to protocol of supplier (Roche Diagnostics, US). Precipath (Standardized serum Roche Diagnostics, US) was used as internal standard.

Statistical analysis

Data are expressed as mean ±SEM. A 2-tailed Student's t-test was used to compare individual groups in the in vivo studies. A level of $P<0.05$ was considered significant.

Results

No effect of FcεRIβ^{+}-cell depletion on body weight, total cholesterol and leukocyte counts in RMB-apoE$^{-/-}$ mice

A schematic overview of the current study is depicted in figure 1a. In short, FcεRIβ^{+} cells were depleted in RMB-apoE$^{-/-}$ mice before induction of atherosclerosis by western type diet feeding. DT efficiency was determined by flow cytometry analysis for circulating blood basophils. At 3 days after the last DT injection, we observed a population of basophils in PBS treated mice and absence of basophils in the DT treated group (Fig. 1b). Subsequently, mice were fed a western type diet for a total of 6 weeks, two weeks after start of diet mice received perivascular collars to accelerate lesion development. At sacrifice, we did not observe weight differences between the PBS and the DT treated group (Fig. 1c). Total serum cholesterol level (Fig. 1d), total leukocyte and red blood cell numbers, as well as platelet counts (Fig. 1e) did not differ between the mast cell depleted and control treated group.

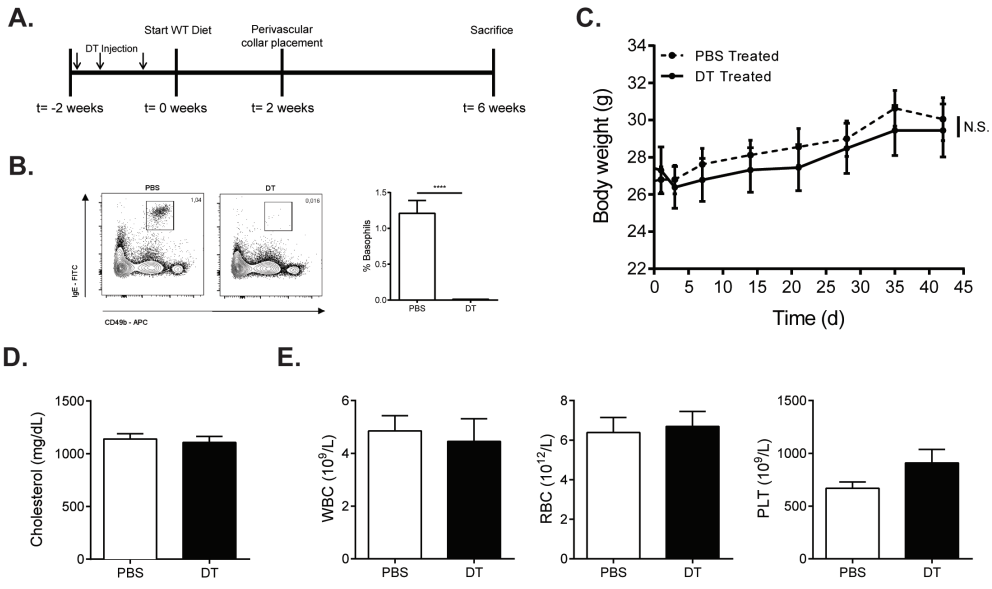

Figure 1. The effect of FcεRIβ^{+}-cell depletion on body weight, total cholesterol and leukocyte counts in RMB-apoE$^{-/-}$ mice

(A) Flow-chart of the in vivo experimental set-up. (B) Gating stratagy of blood basophils and summary of all PBS and DT treated mice. (C) Body weight was monitored during the experiment in PBS- or DT-treated RMB-apoE$^{-/-}$ (n=15/group). (D) Total serum cholesterol levels were determine in PBS- or DT treated RMB-apoE$^{-/-}$ mice at the end of the experiment (n=15/group). (E) Total white blood cell (WBC), red blood cell count (RBC) and platelet count was determined in PBS or DT-treated RMB-apoE$^{-/-}$ mice at sacrifice (n=15/group). ***P<0.001.

Depletion of FcεRIβ⁺ cells reduces lesion size and increases lesion stability in carotid arteries.
Atherosclerotic lesion size and composition in the carotid arteries was analyzed after 4 weeks of lesion development. Mast cells are the only tissue resident cells that express the β-chain of the FcεRI [20]. DT treated RMB-apoE$^{-/-}$ mice showed a complete absence of mast cells, while mast cells were present in PBS-treated RMB-apoE$^{-/-}$ mice (Fig. 2a). Quantification of the atherosclerotic lesion size in the carotid artery showed that depletion of FcεRIβ^{+} cells led to a 28% reduction in mean lesion size compared to PBS-treated mice (DT: 78.6 ± 7.9*10^{3} μm^{2} versus PBS: 109.1 ± 8.3*10^{3} μm^{2}, p=0.02, Fig. 2b). Additionally, we analyzed the collagen content using a Sirius Red staining and the percentage of necrotic area as a measure for plaque stability. Depletion of FcεRIβ^{+} cells resulted in an increased collagen content in the lesions of DT-treated mice compared to PBS-treated animals (DT: 10.7 ± 1.1% versus PBS: 4.7 ± 0.7%, p=0.0003, figure 2c) and a reduction in the relative necrotic core area (DT: 32.3 ± 4.3% versus PBS: 44.9 ± 4.3%, p=0.02, Fig. 2d).

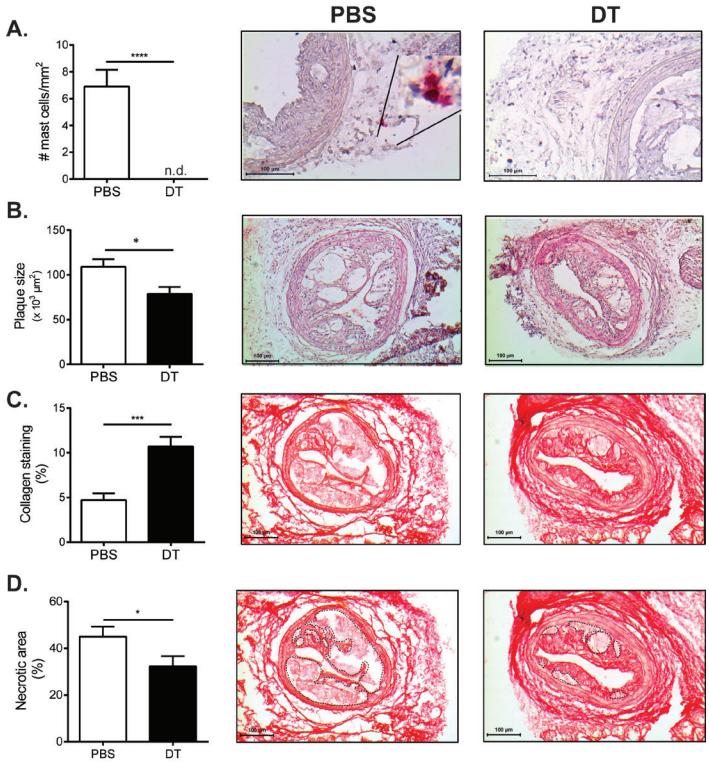

Figure 2. Depletion of FcεRIβ^{+} cells reduces lesion size and increases lesion stability in carotid arteries.
(A) An efficient depletion of perivascular mast cells was observed in DT-, but not in PBS treated RMB-apoE$^{-/-}$ mice (n=15/group). Magnification insert shows mast cells. (B) DT treatment resulted in a reduction in lesion size compared to non-depleted mice (n=15/group). The depletion of FcεRIβ^{+}-cells prior to induction of lesion development coincided with an increase in collagen content (C) and a reduction in necrotic core area (D) compared to non-mast cell-depleted mice (n=15/group). (D: dotted lines indicate necrotic core). *P<0.05, ***P<0.001.

FcεRIβ⁺ cell depletion does not influence lesion size but increases collagen content in aortic root.

Similarly as in the carotid arteries, we observed a complete depletion of perivascular mast cells in the aortic root of DT-treated mice (Fig. 3a). Analysis of the lesion size in the aortic root of PBS and DT treated mice did not reveal any difference in Oil-Red-O positive area (DT: 4.7 ± 0.5*10^5 µm^2 versus PBS: 4.1 ± 0.2*10^5 µm^2, p=NS, Fig. 3b). The collagen content in the lesions of FcεRIβ⁺ cell depleted mice was increased compared to mast cell competent mice (DT: 16.6 ± 1.6% versus PBS: 9.1 ± 1.6% p=0.006, Figure 3c). We observed a trend towards a reduction in necrotic core area in FcεRIβ⁺ cell depleted mice (Fig. 3d).

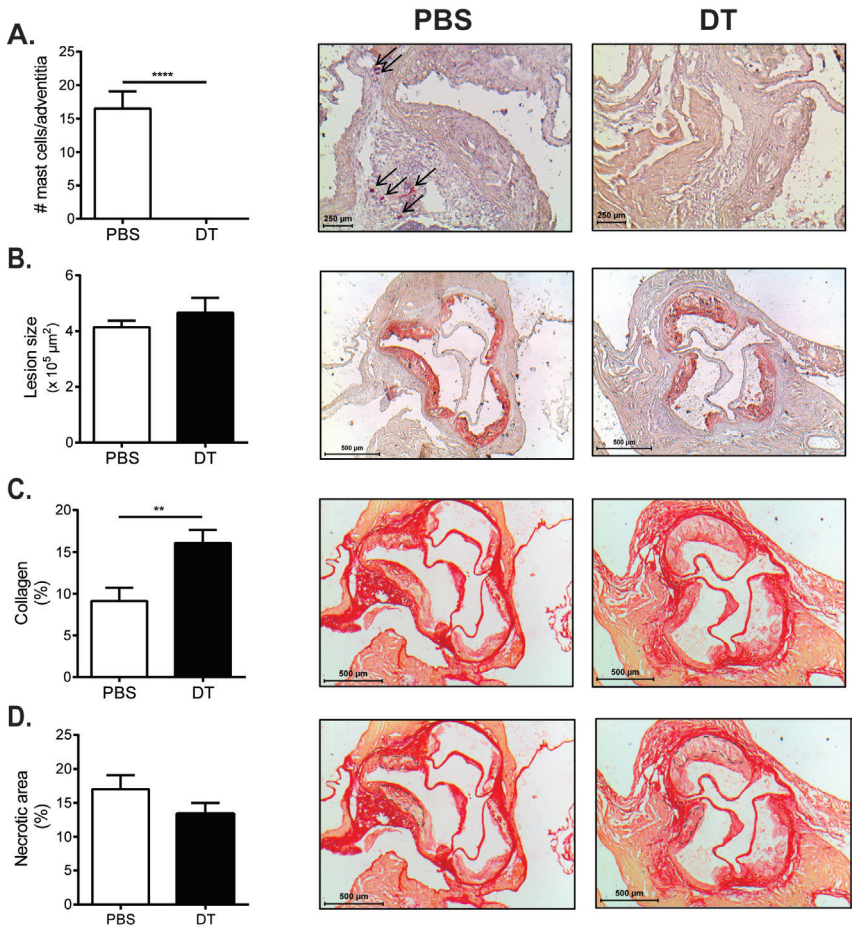

Figure 3. FcεRIβ⁺ cell depletion does not influence lesion size but increases collagen content in aortic root.

(A) An efficient depletion of adventitial mast cells was observed in DT injected RMB-apoE$^{-/-}$ mice (n=15/group) Arrows indicate mast cells. (B) Despite the efficient FcεRIβ⁺-cell depletion, no effect was observed on lesion size between both groups. (C) Collagen content was significantly increased whereas the necrotic core area. (D) was slightly decreased in FcεRIβ⁺-cell deleted mice compared to non-depleted mice. **P<0.01 ****P<0.0001.

At sacrifice, flow cytometry was performed on the WBC population to determine the numbers of circulating innate immune cells such as basophils, neutrophils, (inflammatory) monocytes (Fig. 4a) and adaptive immune cells such as $CD4^+$ T cells, $CD8^+$ T cells and B cells (Fig. 4b). As depicted, we did not detect any difference in the analyzed leukocyte subsets between PBS and DT treated mice.

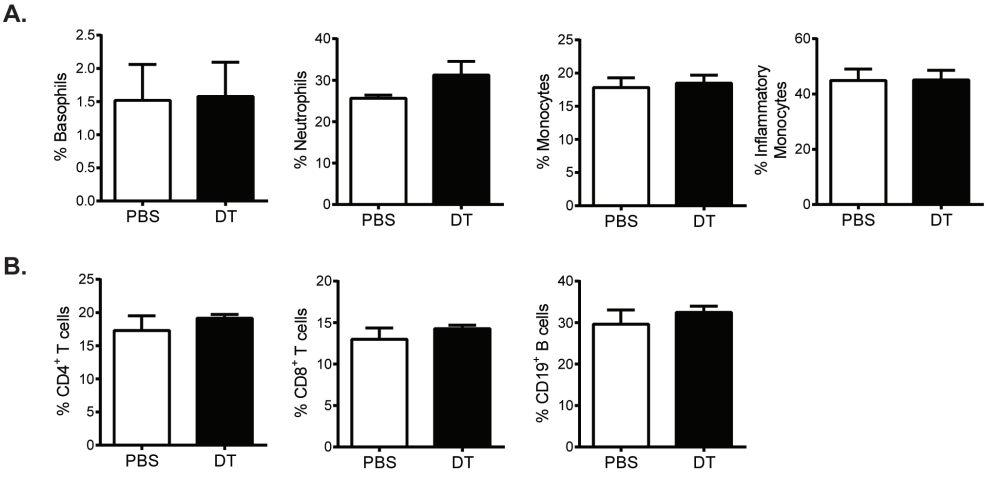

Figure 4. Depletion of FcεRIβ$^+$ cells had no effect on circulating leukocytes in the blood.
(A) Circulating innate basophils ($CD49b^+/IgE^+/CD3^-/CD19^-$), Neutrophils (CD11b/Ly6G), Monocytes ($CD11b^{high}/Ly6G^-/NK1.1^-$), Inflammatory monocytes ($CD11b^{high}/CCR2^+/Ly6C^+/Ly6G^-/NK1.1^-$) and (B) adaptive $CD4^+$ T cells, $CD8^+$ T cells and B-cells ($CD19^+$) in both PBS and DT treated RMB-$apoE^{-/-}$ mice (n=15/group).

Depletion of FcεRIβ⁺ cells decreases levels of pro-atherogenic cytokines and increases total IgE levels.

In the serum we determined pro-atherogenic mediators such as IL-6, TNFα and MCP-1 and as well as total IgG and IgE levels. Circulating IL-6 levels were reduced upon depletion of mast cells (DT: 218.9 ± 22.7 pg/mL versus PBS: 409.2 ± 40.8 pg/mL, p=0.006), and also TNFα levels were reduced (DT: 69.0 ± 5.9 pg/mL versus PBS: 91.9 ± 6.9 pg/mL, p=0.02). No differences in circulating MCP-1 were detected between groups. Total IgG levels in serum did not differ between FcεRIβ⁺ cell competent and FcεRIβ⁺ cell depleted mice. However, we did observe an elevated concentration of total IgE in the serum of FcεRIβ⁺ cell depletedmice (DT: 1024.0 ± 28.5 pg/mL versus PBS: 840.8 ± 80.2 pg/mL, p=0.04).

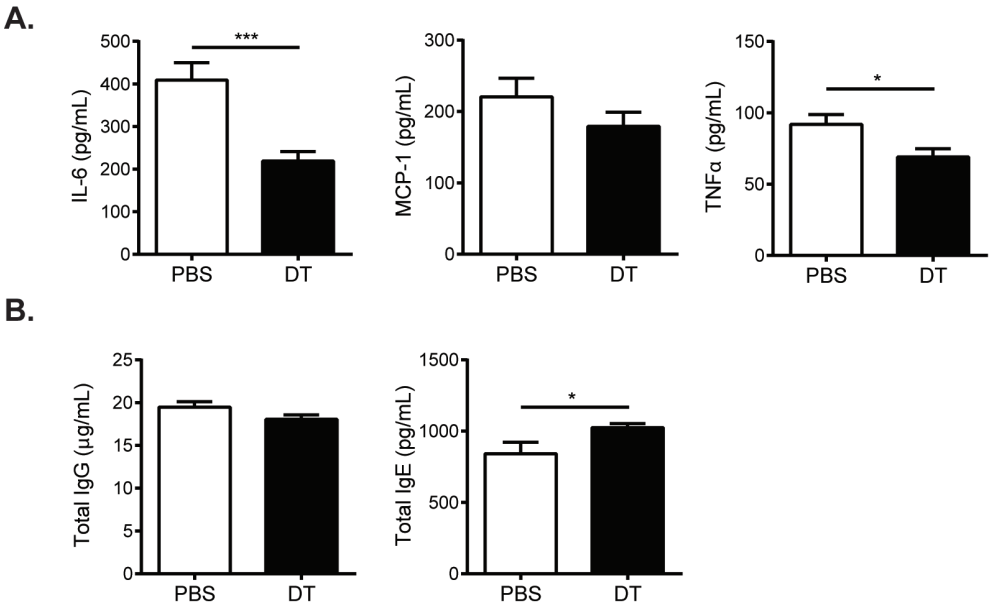

Figure 5. Depletion of FcεRIβ⁺ cells decreases levels of pro-atherogenic cytokines and increases total IgE levels.

(A) Serum levels of IL-6, TNFα and MCP-1 were quantified in serum of PBS and DT treated RMB-apoE$^{-/-}$ mice (n=15/group). (B) Serum levels of total immunoglobulin G (IgG) and immunoglobulin E (IgE) (n=15/group). *P<0.05, ***P<0.001.

Discussion

Mast cells are tissue resident cells located at sites that are in close proximity with the external world like the skin or within the gut [1]. Furthermore, mast cells are located around blood vessels and can influence vascular homeostasis by the release of several mediators, such as proteases, chemokines and cytokines. [4]. Already 60 years ago, mast cells have been implicated in cardiovascular diseases among which atherosclerosis [22]. Many experimental studies have been performed to unravel the contribution of the mast cell and its mediators to plaque initiation, progression and destabilization [11, 12, 23–25]. However, these studies were generally performed in mice with mutations in the stem cell factor signaling (SCF) pathway, like the $Kit^{W\text{-}sh/W\text{-}sh}$ mice, in which a chromosomal inversion causes a disruption of the c-kit (SCF receptor) gene thereby blocking kit expression [13]. Since mast cells need SCF signaling for their maturation, proliferation and survival, these mice lack mast cells [26]. However, it became evident that SCF is also essential for other (non)-immune cells and, as a consequence, these mice suffer from side-effects such as neutrophilia [15]. In the current study we used the recently generated red-mast cell basophil (RMB) mouse strain, which is independent of c-kit [19]. These mice express the DT receptor under control of the promoter of the FcεRIβ-gene, which is expressed exclusively by basophils and mast cells. Nonetheless, there is a marked difference in the repopulation kinetics reported of these cells after depletion.

At sacrifice, we confirmed this difference in repopulation kinetics as blood basophils were completely repopulated while a complete depletion of tissue resident mast cells was still observed in DT treated animals at 6 weeks after depletion of $FcεRIβ^+$ cells. Moreover, the contribution of basophils to atherogenesis is still largely unknown. Basophils have up to now not been demonstrated to be present within the atherosclerotic lesion, which could be caused by their limited lifespan due to early apoptosis outside the bloodstream [27]. Furthermore, we started the $FcεRIβ^+$ cell depletion 14 days before start of western-type diet, and thus the induction of atherosclerotic lesion development, and 4 weeks before perivascular collar placement around the carotids. Therefore, we can conclude that the observed effects of $FcεRIβ^+$ cell depletion on atherogenesis in this study are most likely due to the depletion of tissue-resident mast cells rather than the relative short absence of circulating basophils.

A stable atherosclerotic plaque is characterized by the presence of a relatively small necrotic core, which is covered by a thick layer of smooth muscle cells that produce extracellular matrix molecules such as collagen. In the current study depletion of mast cells had no effect on body weight, total cholesterol and total leukocyte count as it was comparable to PBS control mice. However, we did observe that mast cell depletion resulted in a significant reduction in lesion size and an increase in collagen content in both carotid artery and aortic root lesions. Furthermore, the necrotic core area was significantly reduced in the carotid arteries and a similar trend was observed in the aortic root in mast cell depleted mice. These observations are in line with a previous study that showed that

in LDLr$^{-/-}$Kit$^{W\text{-}sh/W\text{-}sh}$ mice lesions are smaller with a higher collagen content after 12 weeks of diet [12]. Mast cell derived IL-6 and IFNγ have been identified to be the key mediators in lesion development that study. In addition, we have previously shown that inhibition of chymase, one of the mast cell specific proteases, was able to reduce plaque progression in apoE$^{-/-}$ mice, which coincided with enhanced collagen content and decreased necrotic core size [28]

In our current study we detected a reduction in serum IL-6 in mast cell depleted mice. IL-6 promotes endothelial dysfunction, SMC proliferation and migration as well as recruitment and activation of inflammatory cells, thereby accelerating vascular inflammation [29]. Additionally, it was previously demonstrated that IL-6 affects the expression of scavenger receptors SR-A and CD36, which are involved in the uptake of oxLDL and thus promotes the formation of foam cells, a hallmark of early atherosclerotic lesion formation [30]. However, in vivo data discussing IL-6 in atherogenesis are rather contradictory. On one hand it was shown that administration of recombinant IL-6 to apoE$^{-/-}$ mice results in accelerated atherosclerosis, which coincided with an increase in inflammatory cytokines [31]. On the other hand, apoE$^{-/-}$ mice deficient for IL-6 developed larger lesions compared to apoE$^{-/-}$ controls. These studies indicate that IL-6 has both pro- and anti-inflammatory functions in atherosclerosis and that these functions are tightly balanced, which is essential for the immune response outcome during lesion development.

Furthermore, TNFα is an important acute phase cytokine that is implicated in many autoimmune disease such as rheumatoid arthritis and also in atherosclerosis. TNFα is expressed predominantly by activated macrophages but also by many other local (immune) cells like foam cells, smooth muscle cells and mast cells [32–34]. Since macrophages and mast cells have either transmembrane bound TNFα or preformed TNFα in their granules these cells are able to rapidly release TNFα upon stimulation [34–36]. Therefore, mast cells can be a source of TNFα in acute phase reactions [34]. TNFα stimulates both macrophages and smooth muscle cells to synthesize matrix proteases resulting in degradation of the fibrous cap [37, 38]. Moreover, TNFα is capable of decreasing the suppressive capacity of Tregs [39] and mast cell derived TNFα was shown to drive both the hypertrophy of the draining lymph nodes and recruitment T cells to the site of infection [40]. In our study, the depletion of mast cells coincided with a significant reduction in serum TNFα. Sun et al. described that mast cell derived TNFα did not affect atherogenesis [12]. However, TNFα$^{-/-}$ bone marrow derived mast cells used in that particular study produced relatively higher amounts of both IL-6 and IFNγ, i.e. 50 and 30% respectively, compared to wild-type bone marrow derived mast cells. Therefore it cannot be excluded that the observed effects on lesion size are due to enhanced secretion of these proatherogenic cytokines. Furthermore, it has been shown that mice deficient for both apoE$^{-/-}$ and TNFα developed a marked reduction in lesion size, which indicates an active involvement of TNFα in atherogenesis [41].

Taken together, this study establishes that absence of mast cell before the induction of

atherosclerosis is beneficial for both lesion growth and stability as well as for the systemic inflammatory milieu. Our data are correspond with previous experimental atherosclerosis studies demonstrating a critical role for mast cells in atherogenesis, without effects on other hematopoietic cells and shows that the RMB-apoE$^{-/-}$ mouse model can be of great value to study the role of mast cells in atherosclerosis.

References

1. Galli SJ, Kalesnikoff J, Grimbaldeston MA, Piliponsky AM, Williams CMM, Tsai M (2005) Mast cells as "tunable" effector and immunoregulatory cells: recent advances. Annu Rev Immunol 23:749–786
2. Marshall JS (2004) Mast-cell responses to pathogens. Nat Rev Immunol 4:787–799
3. Suurmond J, van der Velden D, Kuiper J, Bot I, Toes REM (2015) Mast cells in rheumatic disease. European Journal of Pharmacology. 2016;778:103-115
4. Bot I, Shi G-P, Kovanen PT (2015) Mast Cells as Effectors in Atherosclerosis. Arterioscler Thromb Vasc Biol 35:265–271
5. Kovanen PT (2007) Mast cells: multipotent local effector cells in atherothrombosis. Immunol Rev 217:105–122
6. Kovanen PT, Kaartinen M, Paavonen T (1995) Infiltrates of activated mast cells at the site of coronary atheromatous erosion or rupture in myocardial infarction. Circulation 92:1084–1088
7. Lappalainen J, Lindstedt KA, Oksjoki R, Kovanen PT (2011) OxLDL-IgG immune complexes induce expression and secretion of proatherogenic cytokines by cultured human mast cells. Atherosclerosis 214:357–363
8. Lee-Rueckert M, Kovanen PT (2006) Mast cell proteases: physiological tools to study functional significance of high density lipoproteins in the initiation of reverse cholesterol transport. Atherosclerosis 189:8–18
9. Kovanen PT (2007) Mast cells and degradation of pericellular and extracellular matrices: potential contributions to erosion, rupture and intraplaque haemorrhage of atherosclerotic plaques. Biochem Soc Trans 35:857–861
10. Wang Y, Shiota N, Leskinen MJ, Lindstedt KA, Kovanen PT (2001) Mast cell chymase inhibits smooth muscle cell growth and collagen expression in vitro: transforming growth factor-beta1-dependent and -independent effects. Arterioscler Thromb Vasc Biol 21:1928–1933
11. Bot I, de Jager SCA, Zernecke A, Lindstedt KA, van Berkel TJC, Weber C, Biessen EAL (2007) Perivascular mast cells promote atherogenesis and induce plaque destabilization in apolipoprotein E-deficient mice. Circulation 115:2516–2525
12. Sun J, Sukhova GK, Wolters PJ, Yang M, Kitamoto S, Libby P, MacFarlane LA, Clair JM-S, Shi G-P (2007) Mast cells promote atherosclerosis by releasing proinflammatory cytokines. Nat Med 13:719–724
13. Grimbaldeston MA, Chen C-C, Piliponsky AM, Tsai M, Tam S-Y, Galli SJ (2005) Mast cell-deficient W-sash c-kit mutant Kit$^{W\text{-}sh/W\text{-}sh}$ mice as a model for investigating mast cell biology in vivo. Am J Pathol 167:835–848
14. Nigrovic PA, Gray DHD, Jones T, Hallgren J, Kuo FC, Chaletzky B, Gurish M, Mathis D, Benoist C, Lee DM (2008) Genetic Inversion in Mast Cell-Deficient Wsh Mice Interrupts Corin and Manifests as

Hematopoietic and Cardiac Aberrancy. Am J Pathol 173:1693–1701

15. Michel A, Schüler A, Friedrich P, et al (2013) Mast cell-deficient Kit(W-sh) "Sash" mutant mice display aberrant myelopoiesis leading to the accumulation of splenocytes that act as myeloid-derived suppressor cells. J Immunol Baltim Md 1950 190:5534–5544
16. Lilla JN, Chen C-C, Mukai K, BenBarak MJ, Franco CB, Kalesnikoff J, Yu M, Tsai M, Piliponsky AM, Galli SJ (2011) Reduced mast cell and basophil numbers and function in Cpa3-Cre; Mcl-1fl/fl mice. Blood 118:6930–6938
17. Feyerabend TB, Weiser A, Tietz A, et al (2011) Cre-mediated cell ablation contests mast cell contribution in models of antibody- and T cell-mediated autoimmunity. Immunity 35:832–844
18. Dudeck A, Dudeck J, Scholten J, et al (2011) Mast cells are key promoters of contact allergy that mediate the adjuvant effects of haptens. Immunity 34:973–984
19. Dahdah A, Gautier G, Attout T, et al (2014) Mast cells aggravate sepsis by inhibiting peritoneal macrophage phagocytosis. J Clin Invest 124:4577–4589
20. Maurer D, Fiebiger S, Ebner C, et al (1996) Peripheral blood dendritic cells express Fc epsilon RI as a complex composed of Fc epsilon RI alpha- and Fc epsilon RI gamma-chains and can use this receptor for IgE-mediated allergen presentation. J Immunol Baltim Md 1950 157:607–616
21. von der Thüsen JH, van Berkel TJ, Biessen EA (2001) Induction of rapid atherogenesis by perivascular carotid collar placement in apolipoprotein E-deficient and low-density lipoprotein receptor-deficient mice. Circulation 103:1164–1170
22. Constantinides P (1953) Mast cells and susceptibility to experimental atherosclerosis. Science 117:505–506
23. Lagraauw HM, Westra MM, Bot M, Wezel A, van Santbrink PJ, Pasterkamp G, Biessen EAL, Kuiper J, Bot I (2014) Vascular neuropeptide Y contributes to atherosclerotic plaque progression and perivascular mast cell activation. Atherosclerosis 235:196–203
24. Wezel A, Lagraauw HM, van der Velden D, de Jager SCA, Quax PHA, Kuiper J, Bot I (2015) Mast cells mediate neutrophil recruitment during atherosclerotic plaque progression. Atherosclerosis 241:289–296
25. Smith DD, Tan X, Raveendran VV, Tawfik O, Stechschulte DJ, Dileepan KN (2012) Mast cell deficiency attenuates progression of atherosclerosis and hepatic steatosis in apolipoprotein E-null mice. Am J Physiol - Heart Circ Physiol 302:H2612–H2621
26. Iemura A, Tsai M, Ando A, Wershil BK, Galli SJ (1994) The c-kit ligand, stem cell factor, promotes mast cell survival by suppressing apoptosis. Am J Pathol 144:321–328
27. Weber C, Zernecke A, Libby P (2008) The multifaceted contributions of leukocyte subsets to atherosclerosis: lessons from mouse models. Nat Rev Immunol 8:802–815
28. Bot I, Bot M, van Heiningen SH, et al (2011) Mast cell chymase inhibition reduces atherosclerotic plaque progression and improves plaque stability in ApoE-/- mice. Cardiovasc Res 89:244–252
29. Wassmann S, Stumpf M, Strehlow K, Schmid A, Schieffer B, Böhm M, Nickenig G (2004) Interleukin-6 induces oxidative stress and endothelial dysfunction by overexpression of the angiotensin II type 1 receptor. Circ Res 94:534–541
30. Keidar S, Heinrich R, Kaplan M, Hayek T, Aviram M (2001) Angiotensin II administration to atherosclerotic mice increases macrophage uptake of oxidized ldl: a possible role for interleukin-6.

Arterioscler Thromb Vasc Biol 21:1464–1469

31. Huber SA, Sakkinen P, Conze D, Hardin N, Tracy R (1999) Interleukin-6 Exacerbates Early Atherosclerosis in Mice. Arterioscler Thromb Vasc Biol 19:2364–2367
32. Tanaka H, Sukhova G, Schwartz D, Libby P (1996) Proliferating arterial smooth muscle cells after balloon injury express TNF-alpha but not interleukin-1 or basic fibroblast growth factor. Arterioscler Thromb Vasc Biol 16:12–18
33. Jovinge S, Ares MP, Kallin B, Nilsson J (1996) Human monocytes/macrophages release TNF-alpha in response to Ox-LDL. Arterioscler Thromb Vasc Biol 16:1573–1579
34. Gordon JR, Galli SJ (1990) Mast cells as a source of both preformed and immunologically inducible TNF-alpha/cachectin. Nature 346:274–276
35. Horiuchi T, Mitoma H, Harashima S, Tsukamoto H, Shimoda T (2010) Transmembrane TNF-α: structure, function and interaction with anti-TNF agents. Rheumatol Oxf Engl 49:1215–1228
36. Walsh LJ, Trinchieri G, Waldorf HA, Whitaker D, Murphy GF (1991) Human dermal mast cells contain and release tumor necrosis factor alpha, which induces endothelial leukocyte adhesion molecule 1. Proc Natl Acad Sci U S A 88:4220–4224
37. Galis ZS, Muszynski M, Sukhova GK, Simon-Morrissey E, Unemori EN, Lark MW, Amento E, Libby P (1994) Cytokine-stimulated human vascular smooth muscle cells synthesize a complement of enzymes required for extracellular matrix digestion. Circ Res 75:181–189
38. Galis ZS, Muszynski M, Sukhova GK, Simon-Morrissey E, Libby P (1995) Enhanced expression of vascular matrix metalloproteinases induced in vitro by cytokines and in regions of human atherosclerotic lesions. Ann N Y Acad Sci 748:501–507
39. Stoop JN, Woltman AM, Biesta PJ, Kusters JG, Kuipers EJ, Janssen HLA, van der Molen RG (2007) Tumor necrosis factor alpha inhibits the suppressive effect of regulatory T cells on the hepatitis B virus–specific immune response. Hepatology 46:699–705
40. McLachlan JB, Hart JP, Pizzo SV, Shelburne CP, Staats HF, Gunn MD, Abraham SN (2003) Mast cell-derived tumor necrosis factor induces hypertrophy of draining lymph nodes during infection. Nat Immunol 4:1199–1205
41. Brånén L, Hovgaard L, Nitulescu M, Bengtsson E, Nilsson J, Jovinge S (2004) Inhibition of Tumor Necrosis Factor-α Reduces Atherosclerosis in Apolipoprotein E Knockout Mice. Arterioscler Thromb Vasc Biol 24:2137–2142